

Beams affected by corrosion influence of reinforcement placement in the cracking

Néstor F. Ortega^{1a}, Irene E. Rivas^{*2}, Raquel R. Aveldaño^{1a} and María H. Peralta^{2a}

¹Engineering Department, Universidad Nacional del Sur, Av. Alem 1253, (8000) Bahía Blanca, Argentina

²Engineering Faculty, Universidad Nacional del Centro de la Prov, Buenos Aires,
Avda, Del Valle 5737, (7400) Olavarría, Argentina

(Received September 8, 2009, Accepted September 25, 2010)

Abstract. The results of experimental and numerical investigations on reinforced concrete beams, with different longitudinal rebars affected by corrosive processes are presented in this paper. Different diameters and/or different distributions of longitudinal rebars were employed keeping constant the total section in each analyzed case, (maintaining a constant stirrup diameter and distribution). The rebars were subjected to accelerated corrosion in the experimental study. Electrochemical monitoring of the process, periodic measuring of the cover cracking and gravimetry of the rebars were performed through the test. Some building recommendations are obtained in order to be considered by designers of concrete structures. The numerical simulation was carried out through the application of the Finite Element Method (FEM), employing plane models, and using linear-elastic material model. The cracking process was associated with the evolution of the tensile stresses that were originated. This numerical methodology allows the monitoring of the mechanical behavior until the beginning of the cracking.

Keywords: corrosion; concrete; cracking; numerical simulation; experimental study.

1. Introduction

The basic principles of the structural mechanics like equilibrium, resistance and rigidity should be fulfilled when talking about structural design. In addition, the minimization of the environmental impact and the structural durability has been studied in the last decades. The latter is usually taken into account in the codes; it should be in accordance with the useful life of the project as a whole, and it is directly related to the mechanical requirements and those related to its use. The ideal situation for the useful life of a structure occurs when the aging is so slow that the structure keeps a satisfactory level of serviceability throughout its intended useful life, without requiring important investments for its maintenance.

Reinforced concrete is one of the most widespread materials in the construction industry. Good quality concrete (properly prepared, placed, compacted, etc.), has an acceptable resistance to most of the chemically aggressive agents that exist in nature. But in general, for different reasons, its durability is affected; one of the main effects of this degradation is the corrosion of the rebars.

*Corresponding author, Professor, E-mail: irivas@fio.unicen.edu.ar

^aProfessor

Concrete naturally provides a high degree of protection to the steel rebar from corrosion, due to the alkalinity of its pore solution ($\text{pH} > 12.5$). This high alkalinity enables the formation of a passive film on the rebar surface, which prevents the development of an active corrosion process. This passive state can be inhibited by the destruction of the protective film by aggressive ions (chlorides) or by an acidification of the environment in the concrete near the rebar (Hou and Chung 2000, Poupard *et al.* 2006).

The oxides produced by the corrosion of the rebars inside a concrete structure generate pressure over the surrounding concrete that eventually generates cracks in the concrete cover of the steel rebars. This is due to the fact that the volume of the oxide is higher than the iron volume (Alonso *et al.* 1998). These cracks, which run parallel to the rebars, may affect the bearing capacity and service life of the structure (Casal *et al.* 1996). As a consequence, they shorten its effective lifetime, letting the products (oxygen, water and in certain cases, chlorides) reach it easily, contributing to the corrosion of the rebars.

Damage in the concrete resulting from steel corrosion is manifested as expansion, cracking and eventually, peeling of the cover (Andrade *et al.* 1993).

The speed of corrosion (measured by the intensity of current originated in the rebars affected by the corrosion) is the key factor that controls the evolution of cracking (Vidal *et al.* 2004) and, therefore, it is linked with the possibility of safety prediction and residual capacity of the concrete structures in the degradation process (Du *et al.* 2005).

An important number of experimental studies have been conducted to research the rebar corrosion process and its effects on concrete structures, with the emphasis on the concrete cracking and loss of steel-concrete bond (Al-Sulaimani 1992, Andrade *et al.* 1993, Almusallam *et al.* 1996, Alonso *et al.* 1998, Cairo *et al.* 2007, Shayanfar *et al.* 2007).

Different theoretical investigations (Allampallewar and Srividya 2008, Bhargava *et al.* 2006, Vidal *et al.* 2004) and numerical investigations have also been developed using in general the Finite Element Method (Du *et al.* 2006, Zhu and Law 2007).

The present work is the follow up of a line of numerical and experimental investigation where the influence of different geometrical characteristics of the rebars was studied. The purpose is to determine whether reinforced beams with the same section of steel (longitudinal rebar) but with different combinations of diameters and/or distribution of the steel rebar subjected to accelerated corrosion, may experience different behaviors, with regards to the loss of area due to the formation of oxides and the subsequent cracking of the concrete cover. The comparison of the predicted results of the numerical model with the experimental data shows similar results. This offers some useful information for the design of concrete sections.

2. Experimental analysis

2.1 Materials and models

The characteristics of the concrete employed in all beams are shown in Table 1, whereas those of the rebars are defined in Table 2. Ratio $w/c = 0.58$ was adopted in order to improve porosity which enhances wet penetration through concrete to rebars, and corrosion effects may be observed during the research period (about six months).

Table 1 Concrete composition and characteristics

Constitutive materials (kg/m ³ of concrete)	Water Cement ratio	Slump (cm)	Average compressive strength (MPa)	Average tensile strength (MPa)
Portland Cement with calcareous filler CPF40 IRAM 50000	300			
Fine aggregate (natural siliceous sand)	864	0.58	8.00	22.3
Coarse aggregate (shingles MNS 25 mm)	1050			
Drinkable tap water	175			2.0

Table 2 Rebar characteristics

Rebar	Diameter (mm)	Tensile yield strength (MPa)	Tensile ultimate strength (MPa)
Longitudinal	4.2	597	716
	6	530	640
Stirrups	2.1	302	414

IRAM Standards (Norma IRAM-IAS U 500-26 1987 and Norma IRAM-IAS U 500-528 1987) prescribe that chemical composition of the 4.2 mm and 6 mm rebars is not exactly the same. They present differences in the carbon amount in the order of 0.02%, phosphorus in 0.005% and sulphur in 0.005%. It determines that oxides produced on every kind of rebars are practically the same and, therefore, the pressure generated on the concrete are the same too.

During the construction of the concrete beams, an attempt to reproduce, as accurately as possible, similar conditions to the ones that usually occur in practice was made. Therefore, the dimensions of the reinforced concrete beams were chosen so as to keep a geometric equivalence with those used in real construction sites (approximate scale 1:3): 2.20 m length, 0.08 × 0.16 m cross-section. The longitudinal rebar (placed on the top of the beam) was made with an almost constant section in all beams ($S \cong 0.56 \text{ cm}^2$) although each one was materialized in a different way, as it will be specified in Table 3. The non stresses longitudinal rebar (constructive, not bearing, placed on the bottom of the beam) was made with two bars with a nominal diameter of 4.2 mm. Closed stirrups were made with a 2.1 mm nominal diameter wire, with a spacing of 10 cm. The longitudinal rebar cover was also secured by 1 cm isolators.

Concrete was poured into the moulds, mechanically vibrated in three layers and cured during the first 7 days. The beams were kept in laboratory environment (temperature around 20°C, relative humidity around 50%) until the testing time (which took place around a year after the construction of the samples). Cylindrical samples (0.15 × 0.30 m) were also made and then tested, in order to determine their tensile and compressive resistances, in accordance with ASTM-C496-71 Standard (1996).

All the beams were tested without external loads, laying down their full length in order to diminish rebar tension.

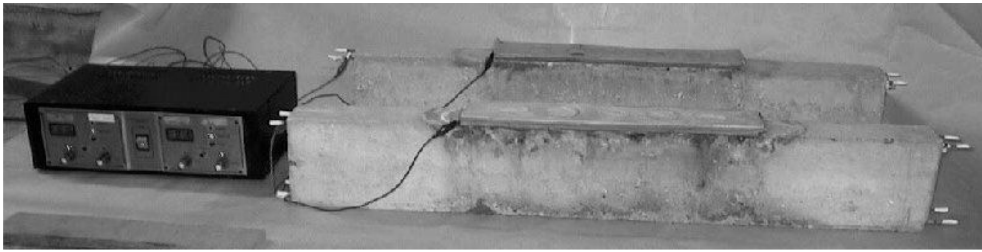


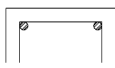
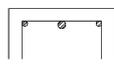
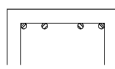
Fig. 1 Beams during the test

2.2 Process of accelerated corrosion

A central portion of the beam's rebars underwent a process of accelerated corrosion during approximately six months through the application of an external current supplied by a galvanostat (initial current density = $100 \mu\text{A}/\text{cm}^2$) (Fig. 1). The current was applied to the concrete's surface on the top of the beams through a counter electrode made with a stainless steel net (50 cm long and the same width as the beam). A sponge of the same dimensions of the net was put over it, and kept wet with a permanently controlled amount of 0.3% (by weight) sodium chloride which increased the medium conductivity. A higher amount was not used in order to avoid the localized attack in the bars that chlorides produce. The beams during the test can be seen in Fig. 1.

This applied current density - $100 \mu\text{A} / \text{cm}^2$ - is approximately ten times higher than that found in highly corroded reinforced concrete structures (Rodríguez *et al.* 1993). It was chosen in order to obtain attack penetrations of some importance in a relatively short time, without altering the nature of the process. For the same reason it was also adopted by other authors (Alonso *et al.* 1998, Casal *et al.* 1996, Acosta and Sagüés 1998).

Table 3 Characterization of the tested beams

Beam denomination	Upper rebar			Stirrups	Current intensity (mA)
	Distribution of steel rebar (mm)	Rebar section (cm^2)	Rebar perimeter (cm)		
B11	$2\text{Ø}6$ 	0.5655	37.70	$1\text{Ø}2.1$ c/10 cm	21.5
B12	$2\text{Ø}4.2+1\text{Ø}6$ 	0.5598	45.24	$1\text{Ø}2.1$ c/10 cm	25.3
B13	$2\text{Ø}4.2+2\text{Ø}4.2$ 	0.5542	52.78	$1\text{Ø}2.1$ c/10 cm	29.0
B14	$4\text{Ø}4.2$ 	0.5542	52.78	$1\text{Ø}2.1$ c/10 cm	29.0

2.3 Tests

An area affected by corrosion was observed on the upper bars formed by their perimeter and 50 cm length as well as that of the stirrups placed in this area up to a vertical length of 1 cm. The characteristics of the tested beams are presented in Table 3, specifying the applied current intensity.

Since the beginning of the moistening and the galvanostatic application of the current density of the test, a daily visual inspection of the beams' surface was done, up to the appearance of the first stains and first cracks. After the cracks appeared, their lengths and widths were periodically measured with a graduated ruler, with a precision of 0.05 mm, in order to find out the cracking areas and their maximum widths. At the same time, the corrosion potentials were registered with a corrosion analyzing instrument specially designed to analyze corrosion in concrete structures, using a reference electrode of copper-copper sulphate (CCS), in order to do an electrochemical monitoring of the phenomenon, which was according to the normalized procedure by ASTM C 876 (1980). Later on, the uncovering of the rebars was done; observing its damage and finally a gravimetry was done in order to determine the particularities of the corrosion registered in each analyzed case.

3. Numerical analysis

In order to verify the experimental determinations, plane models were analyzed through the application of the Finite Elements Method, using the ALGOR FEMS PROGRAM (2007).

3.1 Geometric model

The models indicated in Fig. 2 were studied, considering the same rebar layout as in the experimental model, so as to compare the obtained results using both methods.

For the numerical models, a discretization that considered a densification in the surroundings of the rebars and the thickness of the cover was done, since these would probably be the most mechanically demanded areas. The 2D elastic element was used, with two translational freedom degrees per node. The mesh used in the different analyzed models is shown in Fig. 2.

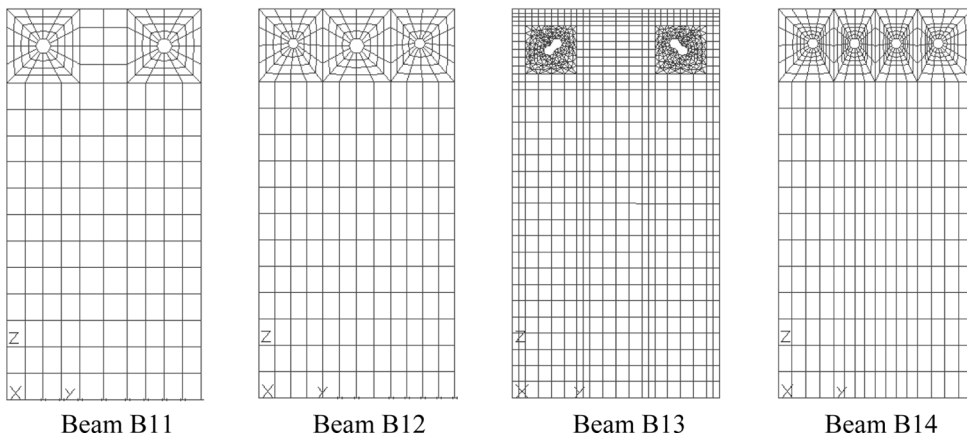


Fig. 2 Discretization of the models

The boundary conditions of the models simulated their continuous support on the low face of the beam.

3.2 Constitutive model

This model was analyzed with the Finite Element Method, using linear-elastic predictions. Even though they do not fully represent the concrete's behavior, especially after cracking, since they prevent from observing the redistribution of stresses once the tensile stress limit is reached in the concrete, they do allow the comparative analysis of the behavior of the different models. Given the analyzed model's range, the study was focused on the distribution of the maximum main stresses and strain, in order to identify the most demanded strained areas, where the cracks may be located, considering the influence of the parameters that are the target of this study.

The characteristics of the concrete that correspond with the ones obtained experimentally, were:

Longitudinal elasticity modulus $E = 28000$ MPa

Poisson coefficient $\mu = 0.2$

Characteristic tensile strength = 2 MPa

Characteristic compressive strength = 17 MPa.

3.3 Model of actions

In the previously described experimental work, the steel rebars were subjected to an accelerated corrosion process through the application of a galvanostatic current under constant moistening with a solution of sodium chloride. Even though the presence of chlorides would indicate the appearing of pitting, a direct correlation between the most pitted places and those with the maximum crack widths did not exist, therefore the corrosion was considered to be uniform.

In the numerical model, the action of the corrosion products over the concrete was simulated through a circumferential incremental pressure, caused by the volume increase in the virgin steel, due to the generation of the corrosion products.

4. Results obtained

4.1 Experimental results

4.1.1 Electrochemical monitoring

The electrochemical behavior analyzed through the study of the corrosion potentials in the four beams, showed few noticeable differences. A pseudo-passivation process was found, which had been already observed in previous works (Acosta and Sagüés 1998), and that was similar to all the beams. Only towards the end of the studied period, a slight difference between the cases was found, but always within the value range of passive potentials (between 0 and -300 mV) (Fig. 3).

4.1.2 Cracking monitoring

In all cases, the beginning of cracking was detected around day 13th of the test (penetration about 0.04 mm) although from that point, the increase in cracking areas showed different behaviors, as shown in Fig. 4. The beams that presented a more uniform distribution of rebars throughout their

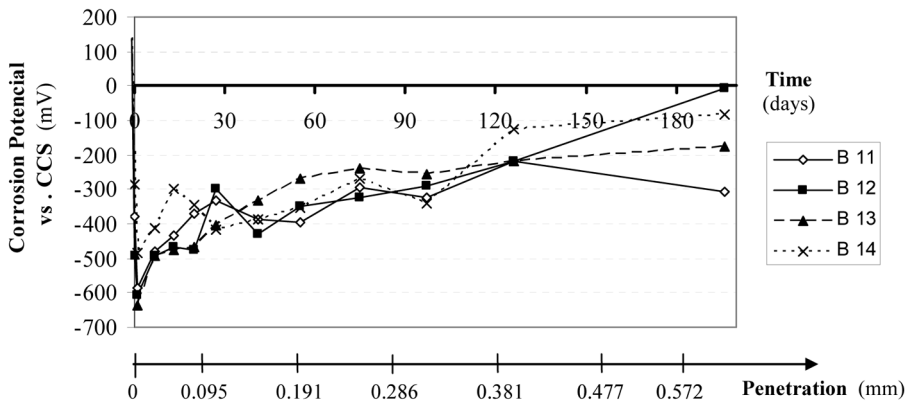


Fig. 3 Monitoring of corrosion potentials (vs. CCS) vs. Time and corresponding attack penetration

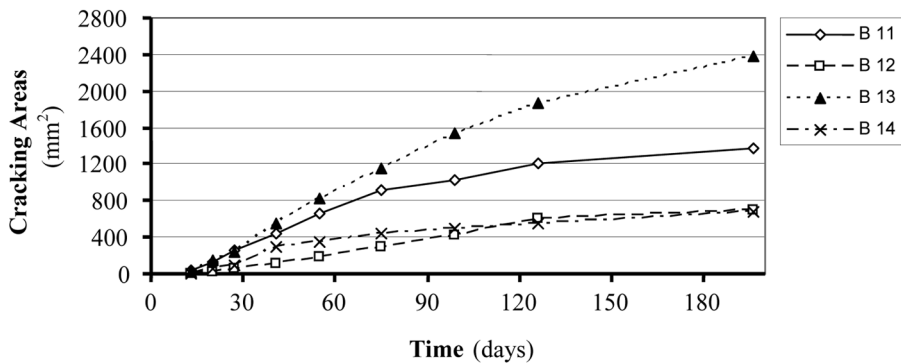


Fig. 4 Variation in cracking areas versus time

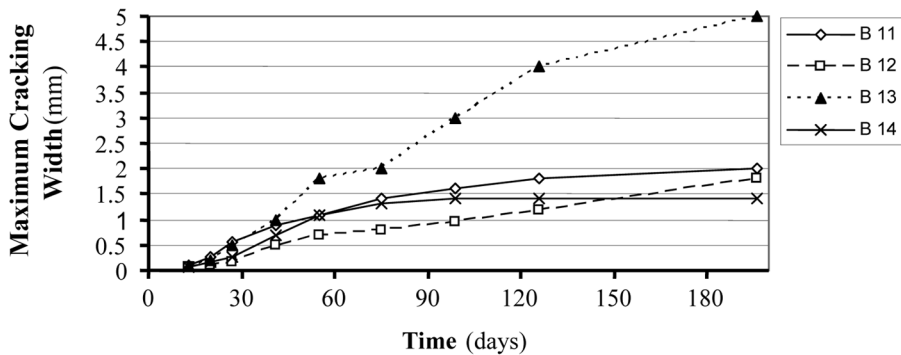
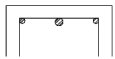
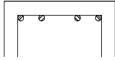


Fig. 5 Variation in maximum cracking width versus time

width (B12 and B14 had a similar behavior, with much less cracking than in the other cases, where the rebars were concentrated on the corners (B11 and B13).

Similar tendencies were found with regards to the maximum cracking widths registered in the studied period (Fig. 5). As it may be seen, beam B13 presents, at the end of the study, a cracking width which is remarkable superior to the other beams.

Table 4 Gravimetric losses in the rebars

Beam	Corroded rebars	Material losses (g)		
		Partial	Total	
 B11	Top rebars	Left	49.50	96.26
		Right	46.76	
	Stirrups		22.10	
 B12	Top rebars	Left	24.66	88.13
		Right	31.66	
		Middle	31.81	
Stirrups		22.43		
 B13	Top rebars	Left 1	20.62	86.07
		Left 2	22.22	
		Right 1	22.46	
		Right 2	20.77	
	Stirrups		34.70	
 B14	Top rebars	Left 1	31.22	94.48
		Left 2	19.20	
		Right 1	18.65	
		Right 2	25.41	
	Stirrups		19.70	

4.1.3 Gravimetry

To complete the study, the concrete was removed from the area affected by corrosion, in order to visualize the condition of the rebars, performing a pitting survey. Then, the gravimetry of the steel rebars was done, in accordance with Standard ASTM G1-67 (2003), whose results are shown in Table 4.

The top face corners were the places that suffered the greatest loss of material (Table 4). This is the case of beams B11 and B13 that had all the rebars concentrated in that corners and showed a greater cracking produced by corrosion (Figs. 4 and 5) as well as more electrochemical activity towards the end of the test (Fig. 3). Likewise, the percentages of losses in beams B12 and B14 corresponding to those bars placed at the top face side, showed higher values than those placed in the middle of the top face. In almost all cases, the cracking produced by corrosion was smaller on the top face, although there was a lot of lateral cracking in the longitudinal rebar direction.

4.2 Numerical results

The experimental results showed that the variation of the cracking areas and the maximum cracking width with the advance of corrosion occurred mostly on the sides of the beams. In this part of the study, it was considered that the Principal Tensile Stress indicates the cracking tendency of

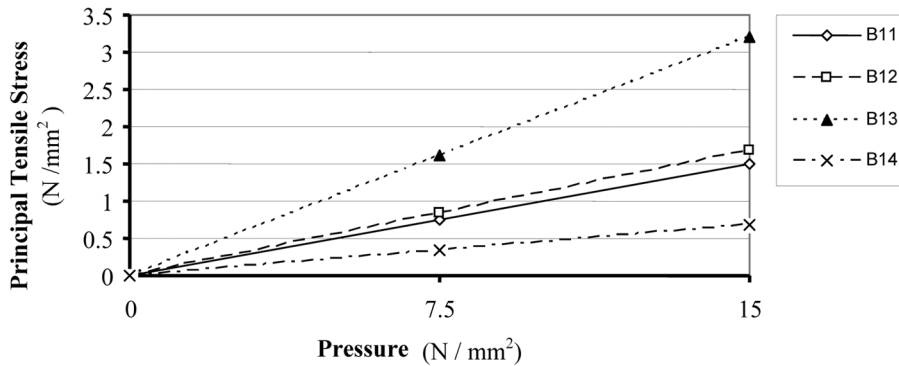


Fig. 6 Variation of principal tensile stress versus pressure on the top face

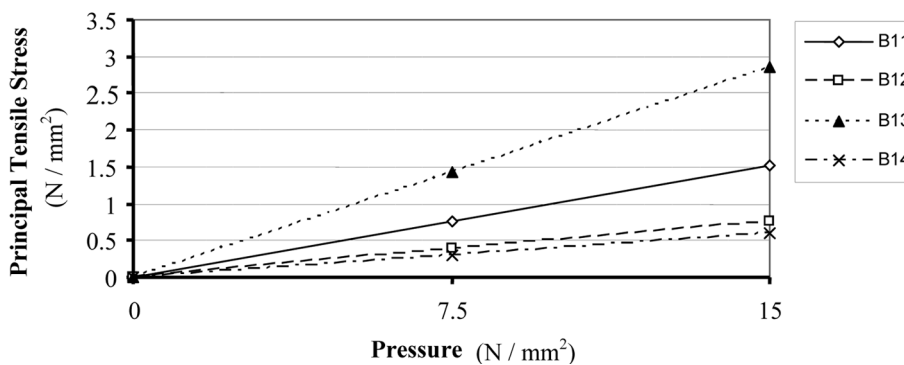


Fig. 7 Variation of principal tensile stress versus pressure on the side face

the models; whereas the pressure increase represents the advancement of the corrosive process with time. In order to obtain results that were comparable with the experimental ones, the variation of the Principal Tensile Stress over the top face and side faces was analyzed, as a function of the pressure generated by the increase of the oxides. The values obtained are presented in Fig. 6 and Fig. 7.

The distribution of the Principal Tensile Stress over a cross-section on the top of the studied beams is shown in Fig. 8, in the different analyzed rebars' layout. The areas where the cracking will be generated, the most mechanically demanded area, may be distinguished besides the values of tensile stress on the top and side faces.

5. Analysis of results

5.1 Analysis of experimental results

Taking into account the different rebar layout, it may be noted that:

- These experiences show that moistening the top face of the beams, in almost all cases, the cracking generated by corrosion was minimal on that face, showing the greatest cracking on the sides, in accordance with the longitudinal rebars. These cracks became a rapid access way for

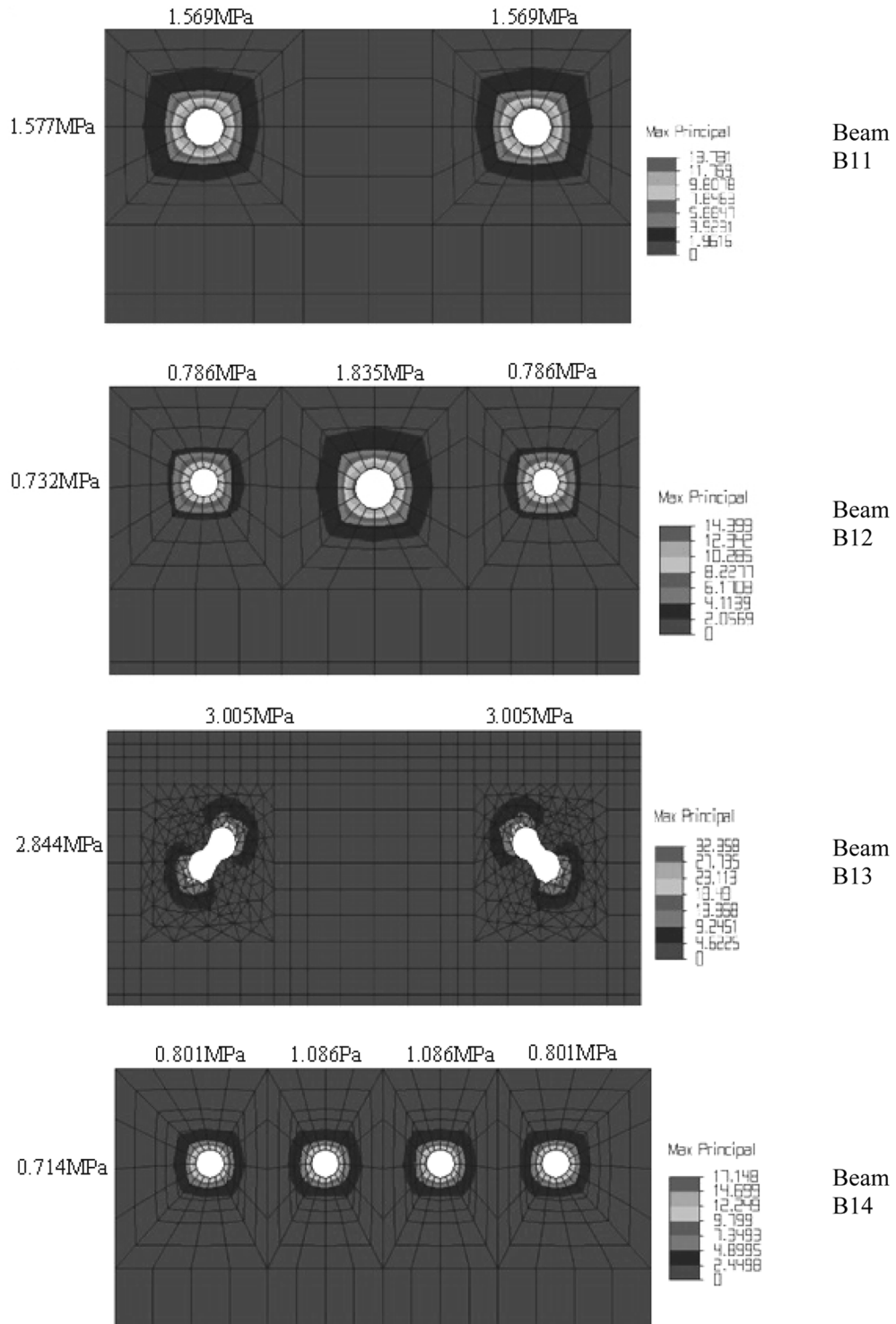


Fig. 8 Distribution of principal tensile stresses

oxygen, accelerating the corrosive process; for that reason, the most serious loss of material took place in the rebars placed on the sides of the beams (Table 4). Such is the case of beams B11 and B13 that showed a higher degree of corrosion cracking (Figs. 4 and 5), presenting a higher electrochemical activity during the last part of the test (Fig. 3). This indicates the convenience of no reinforcing the beams by placing all the steel section on the sides of the beams. It should be noted that in beam B12, cracks also appeared on the top face, in accordance with the middle bar; this type of cracking does not often appear.

- As mentioned, beams B11 and B13, with all the steel rebars concentrated on the top face sides, presented a higher degree of cracking; although a higher loss of material was noticeable (Table 4) on beam B13, especially on the stirrups. This could be the cause of why the stirrups leave the top bars without enough support, allowing the free expansion of oxides and consequently generate a higher degree of cover cracking (Fig. 4).
- From the mechanical point of view, the effect produced by corrosion on the two adjacent rebars (2 Ø 4.2) of beam B13, was larger than its equivalent (1 Ø 6) of beam B11, since the former has a larger perimeter and thus a larger affected surface. It should be noted that, since both rebars were in contact with each other, there might be an overlapping corrosion effect due to differential airing. However, analyzing the results gathered from the numerical and experimental models, the mechanical effects that the latter would produce are of a much smaller magnitude than those caused by the larger perimeter.
- Beams B12 and B14, with a more uniform distribution of the rebars throughout the width of the section, presented similar electrochemical behavior and analogous cracking (Figs. 3, 4 and 5). However, beam B14 had a higher loss of material than beam B12 (Table 4) as expected, since it has a larger attack surface.

Some general observations could be done from the visual inspection of the uncovered rebars and the results of the gravimetry.

The total loss of material, even in the most heavily affected rebars, is not a conclusive indication of the dangerousness of the phenomenon, since pitting appears due to the presence of chlorides. Because of the pitting, the diameters diminished in several scattered sections, up to the breaking of the rebars, weakening the bearing steel section by more than 50% during the tested period.

5.2 Analysis of the numerical results

The analysis of the results obtained from the numerical models leads to the fact that with an equal rebar section (by adopting a disposition that presents a larger rebar surface exposed to the corrosion and/or groups of steel rebars in certain areas), the cracking process that corrosion causes is favored. This may be noticed in Figs. 6 and 7, for example, in model B13, which is the one that presented the highest stress, and therefore the greatest cracking (on the sides).

The numerical study allows knowing the tensional state (before the cracking) on the top face and the side faces of the studied models. Analyzing the curves in Figs. 6 and 7, the different behaviors between models may be seen, on the top and side faces, according to the disposition of the rebars. Over both faces, the highest stresses occurred in B13 -as it was mentioned- and the next highest stress configuration was in B12 and B11. As it also may be seen, there is a great similarity between Figs. 4, 5 and 7, so it is possible to say that the numerical model explains the experimentally registered behavior (cracking) well enough.

6. Conclusions

In accordance with the results obtained from the experimental and numerical studies, the following conclusions may be drawn:

- a) A good coincidence was obtained between the experimental results and the numerical analysis considering linear - elastic predictions, despite the limitations that they impose, which allows a qualitative idea of the behavior of a certain rebar layout, before the beginning of the cracking on the surface of the concrete cover.
- b) In the moistening conditions of the current test, the cracking due to corrosion usually occurs on the sides of the beams, which leads to a greater accessibility of oxygen towards the rebars near those sides, accelerating their corrosive process.
- c) It was seen in the experimental tests as well as in the numerical models that the smallest cracking patterns appeared in the beams which had the highest number of rebars uniformly distributed throughout their cross-section, which is also convenient from the adherence point of view.
- d) The use of groups of rebars (bundled bars) replacing rebars of larger diameter (conserving total area) in the case of eventual corrosive problems is not recommended because, from the mechanical point of view, it is a configuration that generates higher stresses over the concrete mass and, therefore, the cracking will be important; besides, greater corrosion may appear due to differential airing effects.

Conclusions c) and d) will be useful to be considered as guidelines for the design of concrete sections.

Acknowledgements

The experimental part of this work was fully supported by Science and Technology Secretariat of Universidad Nacional del Sur, Bahía Blanca, Argentina, whereas the numerical part was financed by the Science, Art and Technology Secretariat of the Universidad Nacional del Centro de la Provincia de Buenos Aires, Olavarría, Argentina.

The authors would like to thank Studies and Materials Test Laboratory, Soils Laboratory, Structural Models Laboratory, as well as the technicians Mr. Juan Pablo Gorordo and Mr. Diego Smith of the Engineering Department of Universidad Nacional del Sur, for their help during the laboratory tests.

References

- Acosta, A.T. and Sagüés, A. (1998), "Concrete cover cracking and corrosion expansion of embedded reinforced steel", *Proceedings of the 3rd NACE Latin American Corrosion Congress*, 1-15.
- ALGOR SOFTWARE PACKAGE (2007), V.20.3, *Finite Element Modeling Software*, Reference Division, Pittsburgh, Pennsylvania.
- Allampallewar, S.B. and Srividya, A. (2008), "Modeling cover cracking due to rebar corrosion in RC members", *Struct. Eng. Mech.*, **30**(6), 713-732.
- Almusallam, A.A., Al-Gahtani, A.S., Aziz, A.R. and Rasheeduzzafart (1996), "Effect of reinforcement corrosion on bond strength", *Constr. Buil. Mater.*, **10**(2), 123-129.

- Alonso, C., Andrade, C., Rodriguez, J. and Diez, J.M. (1998), "Factors controlling cracking in concrete affected by reinforcement corrosion", *Mater. Struct.*, **31**, 435-441.
- Al-Sulaimani, G.J., Kaleemullah, M., Basunbul, I.A. and Rasheeduzzafar, A. (1992), "Influence of corrosion and cracking on bond behaviour and strength of reinforced concrete members", *ACI Struct. J.*, 220-231.
- Andrade, C., Alonso, C. and Molina, F. (1993), "Cover cracking as a function of bar corrosion: Part 1 - Experimental test", *Mater. Struct.*, **26**, 453-464.
- ASTM C496-71 (1996), "Standard test method for splitting tensile strength of cylindrical concrete specimens", *American Society for Testing and Materials*.
- ASTM C 876 (1980), "Standard test method for half cell potential of reinforcing steel in concrete", *American Society for Testing and Materials*.
- ASTM G1-67 (2003), "Recommended practice for preparing, cleaning, and evaluating corrosion test specimens", *American Society for Testing and Materials*.
- Bhargava, K., Ghosh, A.K., Mori, Y. and Ramanujam, S. (2006), "Model for cover cracking due to rebar corrosion in RC structures", *Eng. Struct.*, **28**, 1093-1109.
- Cairos, J., Du, Y. and Law, D. (2007), "Influence of corrosion on the friction characteristics of the steel/concrete interface", *Construct. Build. Mater.*, **21**, 190-197.
- Casal, J., Diez Arenas, J.M., Rodríguez, J. and Ortega Basagoiti, L. (1996), "Comportamiento estructural de vigas de hormigón con armaduras corroídas", *Hormigón y Acero*, **200**, 113-131.
- Du, Y.G., Clark, L.A. and Chan, A.H.C. (2005), "Residual capacity of corroded reinforcing bars", *Mag. Concr. Res.*, **57**(7), 135-147.
- Du, Y.G., Chan, A.H.C. and Clark, L.A. (2006), "Finite Element Analysis of radial expansion of corroded reinforcement", *Comput. Struct.*, **84**, 917-929.
- Hou, J. and Chung, D.L. (2000), "Effect of admixtures in concrete on the corrosion resistance of steel reinforced concrete", *Corros. Sci.*, **42**, 1489-1507.
- Norma IRAM-IAS U 500-26 (1987), "Alambres de Acero Conformadas para Hormigón", *Instituto Argentino de Racionalización de Materiales Armado*.
- Norma IRAM-IAS U 500-528 (1987), "Barras de Acero Conformadas de Dureza Natural para Hormigón Armado", *Instituto Argentino de Racionalización de Materiales*.
- Poupard, O., L'Hostis, V., Catinaud S. and Petre-Lazar, I. (2006), "Corrosion damage diagnosis of a reinforced concrete beam after 40 years natural exposure in marine environment", *Cement Concrete Res.*, **36**, 504-620.
- Rodríguez, J., Ortega, L.M. and García, A.M. (1993), "Medida de la velocidad de corrosión de las armaduras en estructuras de hormigón, mediante un equipo desarrollado dentro del proyecto Eureka EU 401", *Hormigón y Acero*, **189**, 79-91.
- Shayanfar, M.A., Ghalehnovi, M. and Safiey, A. (2007), "Corrosion effects on tension stiffening behavior of reinforced concrete", *Comput. Concrete*, **4**(5), 403-424.
- Vidal, T., Castel, A. and François, R. (2004), "Analyzing crack width to predict corrosion in reinforced concrete", *Cement Concrete Res.*, **34**, 165-174.
- Zhu, X.Q. and Law, S.S. (2007), "A concrete-steel interface element for damage detection of reinforced concrete structures", *Eng. Struct.*, **27**, 3515-3524.